

doi: 10.12029/gc20200315

田健, 滕学建, 刘洋, 滕飞, 郭硕, 何鹏, 王文龙. 2020. 内蒙古狼山地区早二叠世花岗闪长岩的年代学、地球化学特征及其构造背景[J]. 中国地质, 47(3): 767–781.

Tian Jian, Teng Xuejian, Liu Yang, Teng Fei, Guo Shuo, He Peng, Wang Wenglong. 2020. The chronology, geochemistry of the Early Permian granodiorite in Langshan area, Inner Mongolia and its tectonic setting[J]. Geology in China, 47(3): 767–781(in Chinese with English abstract).

内蒙古狼山地区早二叠世花岗闪长岩的年代学、地球化学特征及其构造背景

田健, 滕学建, 刘洋, 滕飞, 郭硕, 何鹏, 王文龙

(中国地质调查局天津地质调查中心, 天津 300170)

提要:内蒙古狼山山脉西侧分布有大面积的晚古生代岩浆岩, 其时代集中在早石炭世—晚二叠世, 不同时代岩浆岩岩石组合对于认识狼山地区晚古生代构造背景具有重要的意义。文章通过岩石学、岩相学、地球化学及Hf同位素等方法, 对狼山地区查干乃呼都格一带花岗闪长岩体进行了研究。该岩体岩性为花岗闪长岩, LA-ICP-MS锆石U-Pb年龄显示, 其 $^{206}\text{Pb}/^{238}\text{U}$ 加权平均年龄为 $(299\pm 1) \sim (293\pm 2)$ Ma。岩石暗色矿物为角闪石及黑云母, 富含闪长质包体, P_2O_5 含量与 SiO_2 含量之间显示良好的负相关性, 富钠(Na_2O 含量为3.45%~4.96%), 高钠钾比值($\text{Na}_2\text{O}/\text{K}_2\text{O}$ 比值为1.33~2.52), 岩石地球化学特征显示花岗岩成因类型为I型花岗岩。岩石具有负的 $\varepsilon_{\text{Hf}}(t)$ 值(-6.3~-2.0)及 T_{DM2} 为1437~1704 Ma(平均值为1606 Ma), 显示了古—中元古代古老地壳熔融的特点, $\varepsilon_{\text{Hf}}(t)-t$ 及角闪石成因图解显示源区有幔源岩浆参与。花岗岩富集大离子亲石元素Rb、K、Pb, 不同程度的亏损高场强元素Nb、Ta、P、Ti, 轻稀土富集, 重稀土亏损, 弱的负Eu异常, 显示了岩浆弧的地球化学特征。结合晚石炭世—早二叠世狼山地区侵入岩岩石组合为闪长岩+石英闪长岩+花岗闪长岩(英云闪长岩), 早—中二叠世大石寨组火山岩岩石组合为玄武岩+玄武安山岩+安山岩+英安岩, 总体反映了陆缘弧的岩石组合; 狼山地区早二叠世处于大陆边缘弧的构造背景, 与华北地块北缘中东部可以对比。

关 键 词:内蒙古; 狼山地区; 早二叠世; 花岗闪长岩; 大陆边缘弧; 地质调查工程

中图分类号:P588.12⁺¹ **文献标志码:**A **文章编号:**1000-3657(2020)03-0767-15

The chronology, geochemistry of the Early Permian granodiorite in Langshan area, Inner Mongolia and its tectonic setting

TIAN Jian, TENG Xuejian, LIU Yang, TENG Fei, GUO Shuo, HE Peng, WANG Wenglong

(Tianjin Center of China Geological Survey, Tianjin, 300170, China)

Abstract: There exists a large area of Late Paleozoic magmatic rocks on the western side of Langshan Mountain in Inner Mongolia,

收稿日期: 2018-07-15; 改回日期: 2020-05-10

基金项目: 中国地质调查局项目(DD20160039)资助。

作者简介: 田健, 男, 1987年生, 硕士, 工程师, 主要从事区域地质调查及岩浆岩岩石学的研究; E-mail: 243293305@qq.com。

通讯作者: 滕学建, 男, 1980年生, 硕士, 高级工程师, 主要从事区域地质调查及岩浆岩岩石学的研究; E-mail: 451405400@qq.com。

whose ages are concentrated on Early Carboniferous to Late Permian. The magmatic rock assemblages of different ages are of great significance for understanding the Late Paleozoic tectonic background of Langshan area. Based on petrology, petrography, geochemistry and Hf isotopes, this study mainly focused on the granodiorites in Chagannaihuduge zone of Langshan area. LA-ICP-MS U-Pb dating on two granodiorite samples yielded ages of (299 ± 1) Ma and (293 ± 2) Ma respectively. The mafic minerals in granodiorites are dominated by hornblende and biotite. The geochemical data reveal that the granodiorites are of calc-alkaline nature characterized by enrichment of Na_2O (3.45%-4.96%), high $\text{Na}_2\text{O}/\text{K}_2\text{O}$ value (1.33-2.52) and show good negative correlation between P_2O_5 and SiO_2 , which is similar to the characteristics of I-type granites. The Hf isotopic signature for granodiorites and their behavior of elemental geochemical characteristics together indicate that their co-magmatic origin mainly derived from Palaeoproterozoic-Mesoproterozoic continental crust and subordinately from mantle-derived magma. The granodiorites show similar patterns on the chondrite-normalized REE patterns, and display relatively high concentration of light rare earth elements (LREEs) but low content of heavy rare earth elements (HREEs) with minor negative Eu anomalies. The overall chemical similarities of these granodiorites on the primitive mantle-normalized variation diagrams display affinity to arc signature. By combining the large scale regional exposures of diorite+quartz diorite+granodiorite rock assemblage and basalt+basaltic andesite+andesite+anganite in Dashizhai Formation, the authors hold that Langshan area was under the tectonic setting of continental margin arc during Early Permian, similar to that of central-eastern part of NNC.

Key words: Inner Mongolia; Langshan area; Early Permian; granodiorite; continental margin arc; geological survey engineering

About the first author: TIAN Jian, male, born in 1987, engineer, mainly engages in regional geological survey and the study of igneous petrology; E-mail: 243293305@qq.com.

About the corresponding author: TENG Xuejian, male, born in 1980, master, senior engineer, mainly engages in regional geological survey and magmatic rock petrology research; E-mail: 451405400@qq.com.

Fund support: Supported by China Geological Survey Program(No. DD20160039).

1 引言

中亚造山带作为世界上最大的显生宙造山带,横贯东西和南北数千千米(图1a),其复杂的构造演化过程被认为与古亚洲洋的构造运动密切相关(Windley et al., 2007; Han et al., 2011; Xu et al., 2012, 2013; Zhang et al., 2012)。古亚洲洋盆的俯冲增生造山与地体拼贴过程造就了现有的构造格架,形成了大量的古生代岩浆岩(Coleman, 1989; Windley et al., 1990; Allen et al., 1992, 1995; Sengor et al., 1993; Gao et al., 1998; Jahn et al., 2000; Xiao et al., 2004, 2010; Windley et al., 2007; 郭喜运等, 2019; 赵闯等, 2020)。

华北地块北缘位于中亚造山带东南部(图1a),狼山地区则位于华北地块北缘西部(图1b),北侧为中亚造山带,西南侧紧邻阿拉善地块(Wu et al., 1998; Zhang et al., 2013b; 冯丽霞等, 2013),其特殊的构造位置成为了研究古生代构造岩浆演化的有利条件。近年来,随着研究的深入,狼山山脉西侧的岩浆岩成为了研究的热点之一(刘烨, 2012; Peng et al., 2013; Wang et al., 2015, 2016; Liu et al., 2016;

王文龙等, 2017; 滕学建等, 2019),岩体时代集中在早石炭世—晚二叠世(图1b)。然而,目前发现的岩体时代多为早石炭世或者中—晚二叠世,晚石炭世—早二叠世的岩浆岩仅有零星的年代学报道。另外,狼山地区早二叠世的构造背景存在俯冲挤压(刘烨, 2012)及后碰撞伸展等不同的认识(Wang et al., 2015, 2016),这些争议制约了对于狼山地区晚古生代构造岩浆演化过程的认识。

本文基于狼山地区查干呼舒庙等六幅1:5万区域地质调查的基础上,对新识别出的早二叠世早期花岗闪长岩进行岩石学、岩相学、同位素年代学、地球化学及Hf同位素地质等特征的深入研究,进而探讨该期侵入岩的岩石成因及构造背景,为狼山地区晚古生代构造岩浆演化过程提供重要资料。

2 岩体地质概况及岩相学、矿物学特征

2.1 岩体地质概况

早二叠世岩体主要分布在狼山山脉西侧查干乃呼都格一带,在研究区出露面积约5 km²,向南延伸至区外,北侧岩体以早志留世及晚志留世岩体为主(图2)。

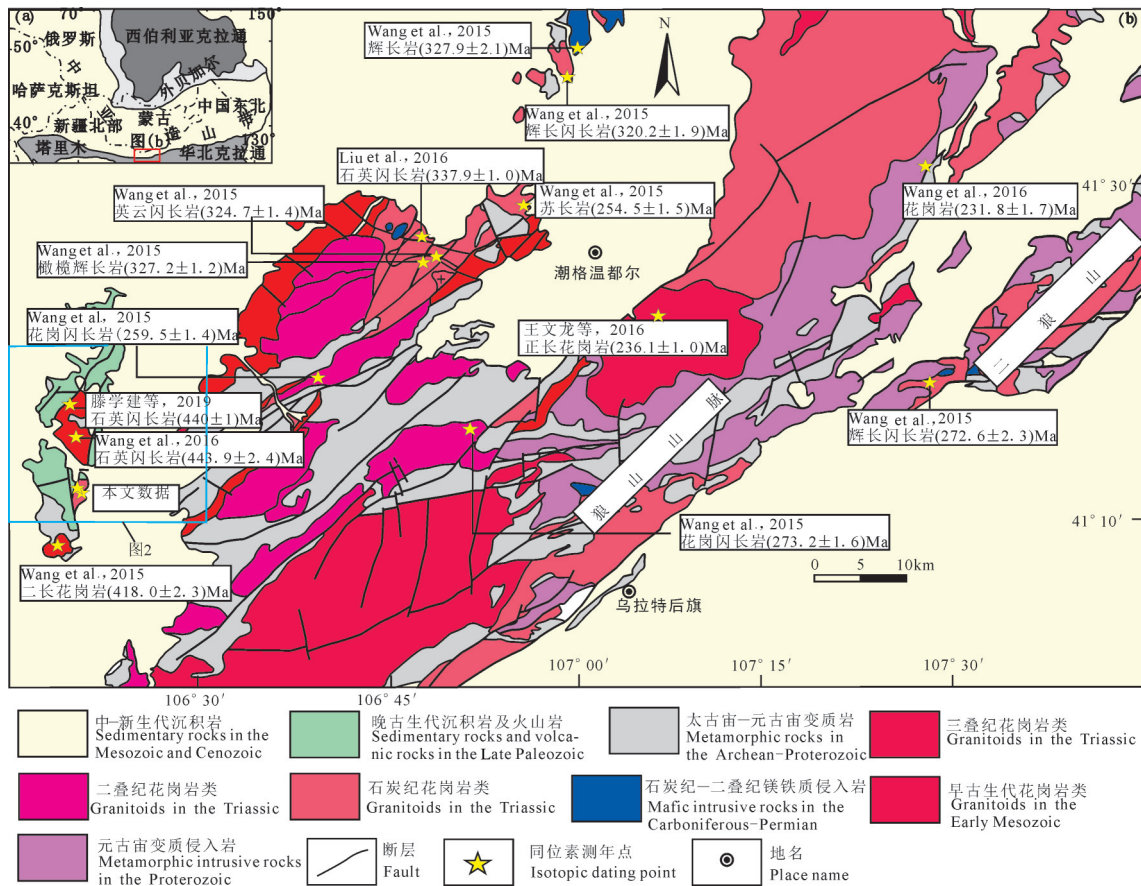


图1 研究区大地构造位置(a);狼山地区侵入岩分布特征(b)(据Wang et al., 2015, 修改)

Fig.1 The tectonic location(a), distribution characteristics of intrusive rocks of the survey area(b)(after Wang et al., 2015)

PM012实测剖面显示(图3),西侧与上石炭统阿木山组为断层接触,东侧侵位于古元古代宝音图岩群大理岩岩组,可见灰白色大理岩的捕掳体。局部被中生代地层或第四纪沉积物覆盖,岩体总体呈近南北向带状展布。黑云母花岗闪长岩构成岩体的主要岩石类型,角闪石花岗闪长岩呈不规则状分布其中,两者为渐变接触关系(图3)。岩石发育块状构造(图4a,c),中粒结构,闪长质包体发育(图4b,d),呈长条状或椭圆状,长轴大小在10~30 cm,岩性为细粒闪长岩,在闪长岩中可见中粒长石晶休,反映了岩浆混合作用的存在。

2.2 岩相学及矿物学特征

灰白色中粒角闪石花岗闪长岩:岩石由斜长石(50%~60%)、钾长石(5%~10%)、石英(20%±)、角闪石(5%~15%)组成(图5a,b),粒径一般2~5 mm,较少量0.3~2.0 mm,个别斜长石直径达6 mm。斜长石主要呈半自形宽板状,杂乱状分布,具绢云母化、高岭土化、褐铁矿化等,隐约见环带构造,局部被钾长石轻微

残蚀状交代。钾长石呈他形粒状,为微斜长石,轻微高岭土化、局部碳酸盐化。石英呈他形粒状,填隙状分布,有的呈堆状聚集分布,粒内具波状、带状消光等。角闪石呈近半自形柱状,绢云母化、褐铁矿化等蚀变。与灰白色中粒角闪石花岗闪长岩不同的是,浅灰红色中粒黑云母花岗闪长岩的暗色矿物为黑云母,钾长石含量有所增加(10%~15%)。

电子探针对花岗闪长岩(TZ5012-1)中的角闪石及斜长石进行了分析(图5c,d),分析结果见表1。

3 分析方法

3.1 电子探针分析

矿物电子探针显微分析在中国地质调查局天津地质调查中心元素分析实验室完成。采用扫描电镜(SEM)对薄片下圈定的矿物进行微区分析,分析结果见表1。

3.2 全岩分析

主量、微量元素和稀土元素分析在中国地质调查局

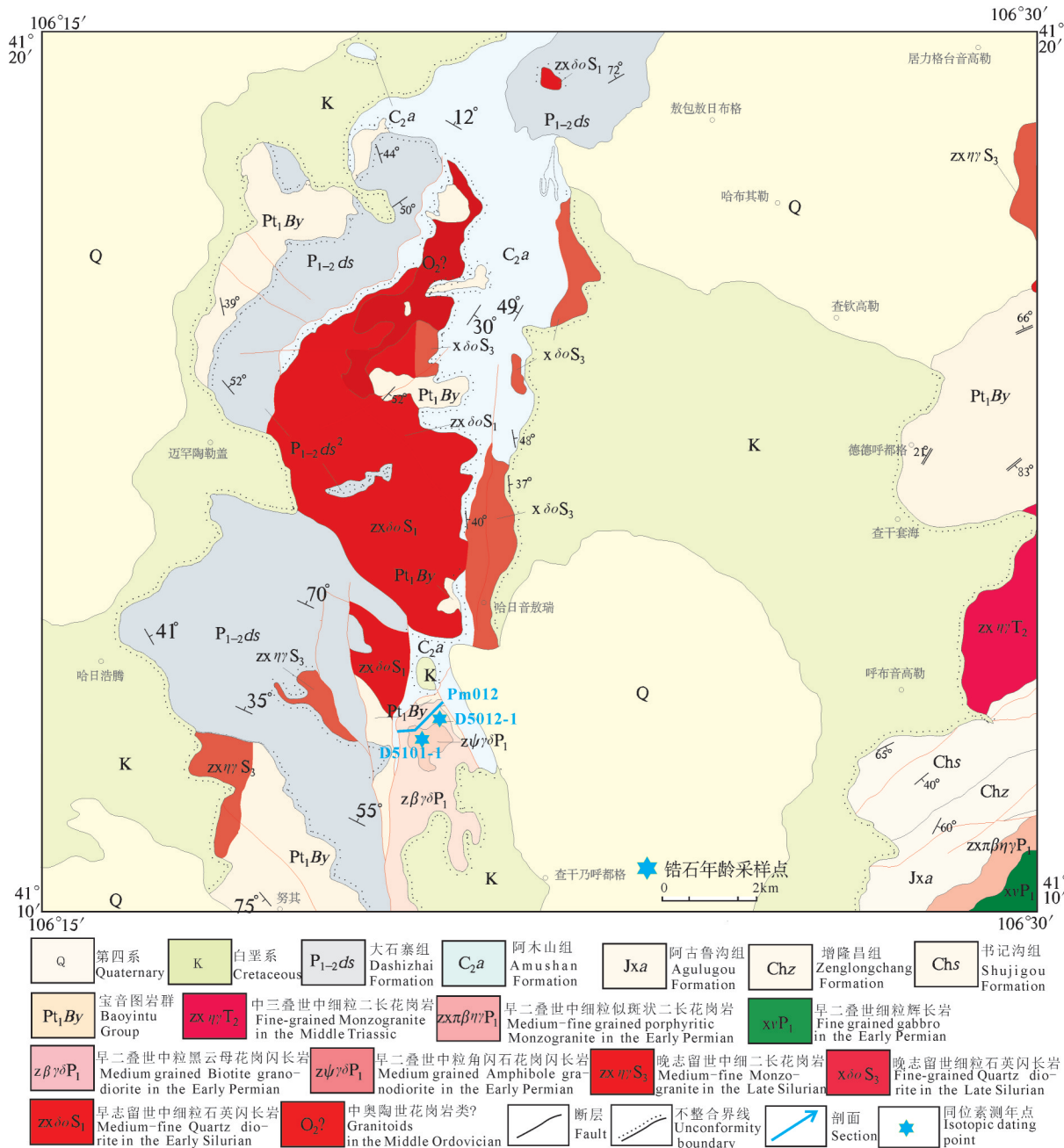


图2 那仁宝力格幅1:5万地质图(据天津地质调查中心^①)

Fig.2 1:50000 geological map of Narenbaolige Sheet (after Tianjin Center of China Geological Survey⁽¹⁾)

天津地质调查中心元素分析实验室完成。将样品熔制成玻璃饼，然后采用X射线荧光光谱仪 XRF-1500 进行主元素测定，分析精度优于1%。称取40 mg 样品于 Tenon 罐中，加入 HNO₃ 和 HF 充分溶解后，用1%的 HNO₃ 稀释后，在 Finigan MAT 公司生产的双聚焦电感耦合等离子质谱仪 (ICP-MS) ELEMENT 上测定微量元素和稀土元素，分析精度优于

5%。分析结果见表2。

3.3 锆石挑选、LA-ICP-MS 年龄测定及锆石原位 Hf 同位素分析

样品无污染碎样和锆石的挑选工作由在河北省廊坊区域地质矿产调查研究所实验室完成。由北京锆年领航科技有限公司制靶，锆石黏贴制成环氧树脂样品靶，经过打磨抛光使锆石露出中心后进

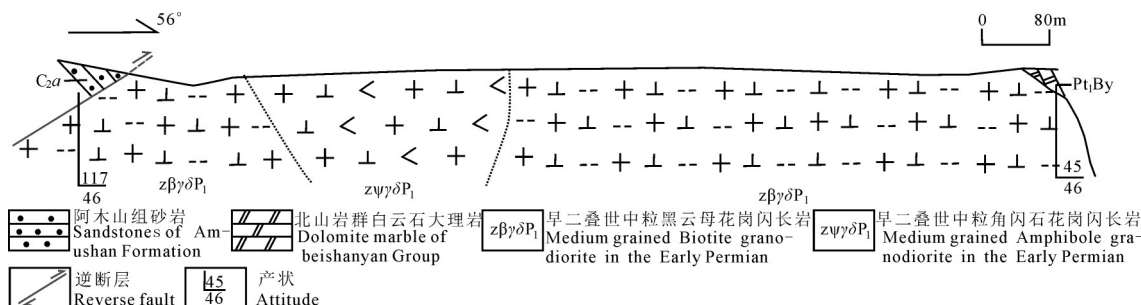


图3 查干乃呼都格一带早二叠世岩体实测剖面(据PM012修改)

Fig.3 The measured section of Early Permian pluton in the Chagannaihude zone (modified from PM012)

行透射光、反射光和阴极发光(CL)显微照相。

锆石U-Pb年代学和Lu-Hf同位素分析在中国地质调查局天津地质调查中心实验室的193 nm激光剥蚀系统(New Wave)和多接收器电感耦合等离子体质谱仪(MC-ICP-MS, Neptune)上完成。U-Pb年代学测试方法见文献(李怀坤等,2010)。采用GJ-1作为外部标准校正锆石的U、Th和Pb同位素分馏:采用NIST610玻璃作为标样计算锆石中U、

Th和Pb含量:利用ICPMSDataCal程序(Liu et al., 2010)和Isoplot程序(Ludwig, 2003)进行数据处理,分析结果见表3。Lu-Hf同位素实验过程中,91500的¹⁷⁶Hf/¹⁷⁷Hf和¹⁷⁶Lu/¹⁷⁷Hf测定结果分别为0.282303±37和0.00030,亏损地幔模式年龄(T_{DM})计算采用Griffin et al. (2003)的推荐值,等离子体质谱实验室方法和同位素分馏校正参考文献Wu et al. (2006),分析结果见表4。

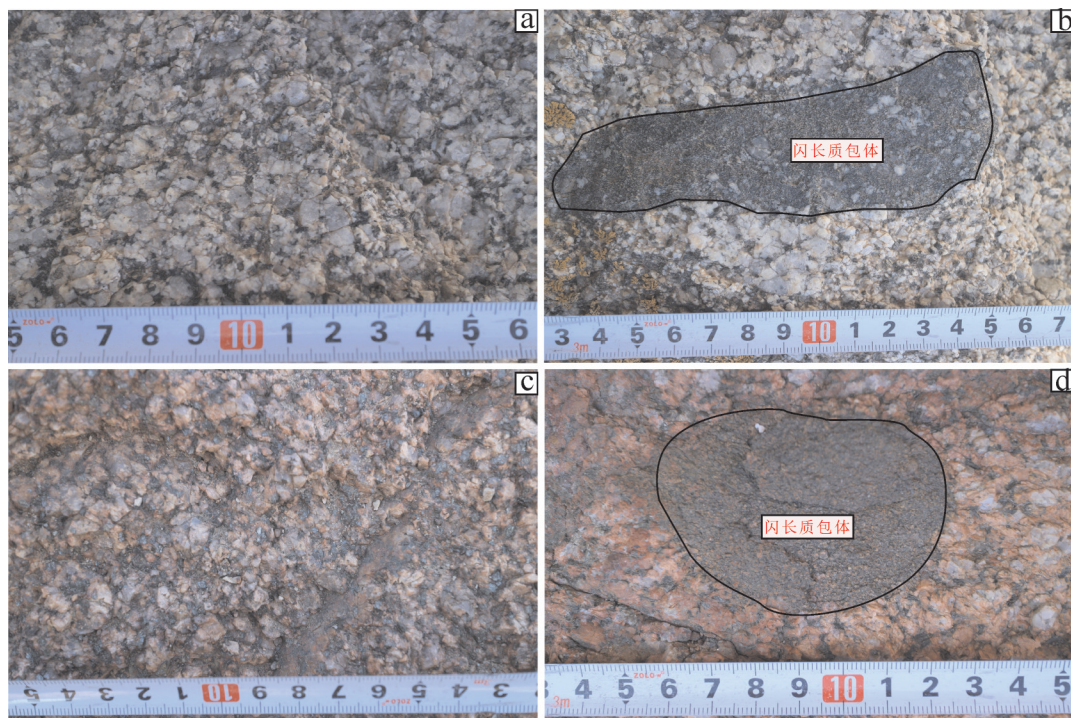


图4 花岗闪长岩的野外露头照片特征

a—灰白色中粒角闪石花岗闪长岩;b—灰白色中粒角闪石花岗闪长岩中的包体;c—浅灰红色中粒黑云母花岗闪长岩;d—浅灰红色中粒黑云母花岗闪长岩中的包体

Fig.4 Outcrop photos and photomicrographs of granodiorite, showing typical textures

a—Gray white medium-grained hornblende granodiorite; b—Enclaves within gray white medium-grained hornblende granodiorite; c—Light gray red medium-grained biotite granodiorite; d—Enclaves within light gray red medium-grained biotite granodiorite

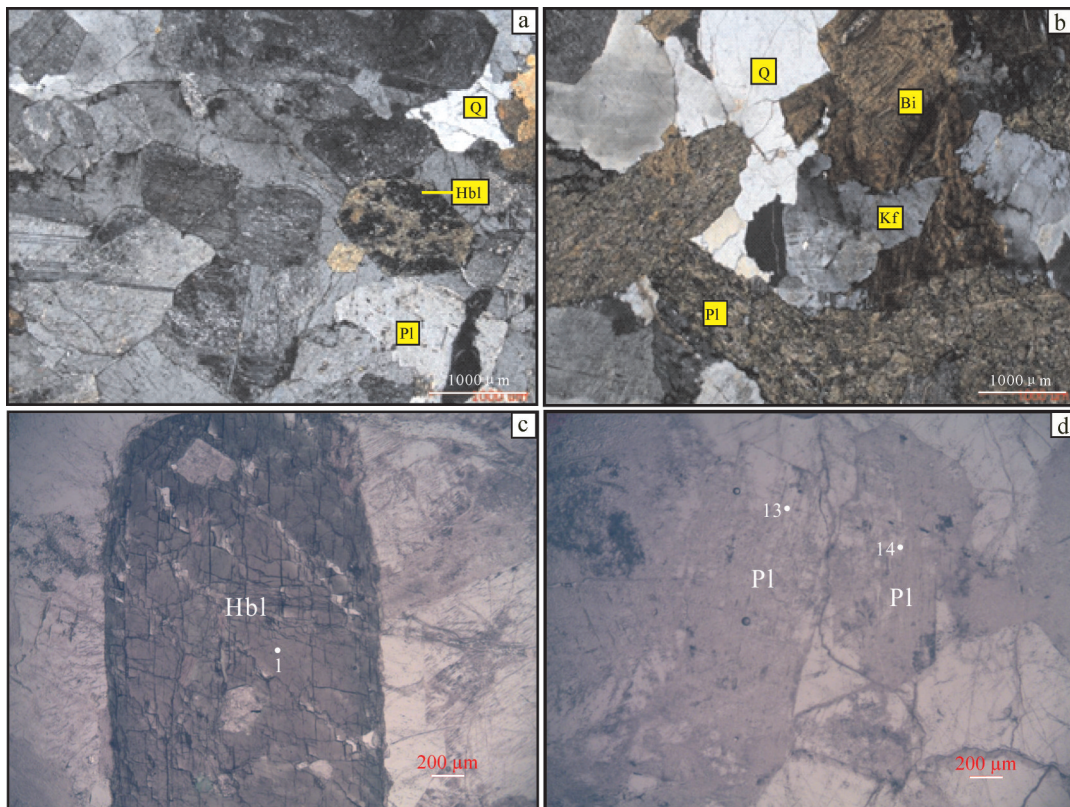


图5 花岗闪长岩显微照片及其电子探针分析矿物与位置

a—灰白色中粒角闪石花岗闪长岩的矿物特征(+); b—浅灰红色中粒黑云母花岗闪长岩的矿物特征(+); c—角闪石矿物特征; d—斜长石矿物特征; Hbl—角闪石; Bt—黑云母; Pl—斜长石; Kf—钾长石; Q—石英; i—角闪石的电子探针位置; 13,14—斜长石的电子探针位置

Fig. 5 Mineralogical characteristics and electron microprobe analysis position of granodiorite

a—Mineralogical characteristics of grayish white medium-grained hornblende granodiorite (+); b—Mineralogical characteristics of light grayish red medium-grained biotite granodiorite (+); c,d—Mineralogical characteristics of hornblende and plagioclase; Hbl—Hornblende; Bt—Biotite; Pl—Plagioclase; Kf—Potash feldspar; Q—Quartz; i—Electron microprobe analysis location of hornblendes; 13,14—Electron microprobe analysis location of plagioclases

4 分析结果

4.1 年代学特征

本次工作对灰白色中粒角闪石花岗闪长岩(TW5012-1)、浅灰红色中粒黑云母花岗闪长岩(TW5101-1)进行了锆石U-Pb年龄测试。所取逐年锆石多呈自形长柱状,表面光滑、干净,锆石CL显(图6a)示其具清晰的韵律环带,长100~200 μm,长宽比为1:1~3:1,具岩浆锆石特征。TW5012-1样品中24个锆石点年龄集中, $^{206}\text{Pb}/\text{U}^{238}$ 加权平均年龄为(299±1)Ma(图6b)。TW5101-1样品中22个锆石点显示出一致的 $^{206}\text{Pb}/\text{U}^{238}$ 加权平均年龄(293±2)Ma;1号点 $^{206}\text{Pb}/\text{U}^{238}$ 年龄为(453±5)Ma,反映了早志留世的岩浆活动,其余2个点(4,23)严重偏离谐合线(图6c),未参与平均年龄计算。

测年结果显示,花岗闪长岩的锆石 $^{206}\text{Pb}/\text{U}^{238}$ 加权平均年龄在误差范围内基本一致,该岩体结晶年龄为(299±1)~(293±2) Ma,侵位于早二叠世。

4.2 地球化学

早二叠世花岗闪长岩SiO₂含量在66.31%~69.57%,FeOT含量在3.07%~4.16%(平均值为3.70%),全碱含量(Na₂O+K₂O)为5.93%~6.93%,Na₂O/K₂O变化于1.33~2.52,Na₂O含量在3.45%~4.96%,显示了富钠的特点。SiO₂-(Na₂O+K₂O)图显示岩石类型为花岗闪长岩(图7a);岩石系列划分图解中显示钙碱性系列(图7b)。

微量元素蛛网图中(图8a),所有样品均具相似的分布型式,富集大离子亲石元素K、Pb,不同程度的亏损高场强元素Nb、Ta、P、Ti,显示了与弧岩浆岩类似的特点。

表1 早二叠世中粒角闪石花岗闪长岩(样品编号5012-1-1)的长石(Pl)及角闪石(Hbl)电子探针数据及分析结果(%)

Table 1 Electron microprobe analyses (%) of Early Permian granodiorite

分析项目	Pl				分析项目	Hbl			
SiO ₂	59.15	69.64	56.85	61.65	SiO ₂	46.35	47.32	45.39	45.15
Al ₂ O ₃	26.45	20.68	27.73	24.95	TiO ₂	1.85	1.6	1.77	1.9
CaO	8.76	1.31	10.38	6.73	Al ₂ O ₃	8.15	7.44	8.16	8.59
Na ₂ O	6.11	10.06	5.26	7.07	FeO	17.75	18.16	19.6	19.1
K ₂ O	0.14	0.07	0.23	0.21	MnO	0.29	0.31	0.43	0.37
BaO	0.01	0.01			MgO	11.44	12.33	10.37	10.43
Si	2.62	2.98	2.54	2.72	CaO	10.88	10.64	10.74	10.78
Al	1.38	1.04	1.46	1.3	Na ₂ O	1.43	1.29	1.24	1.38
Ca	0.42	0.06	0.5	0.32	K ₂ O	0.86	0.63	0.81	0.94
Na	0.53	0.83	0.46	0.6	Cl	0.14	0.09	0.16	0.18
K	0.01	0	0.01	0.01	Si	6.84	6.93	6.8	6.75
Ba	0	0	0	0	Al ^{IV}	1.16	1.07	1.2	1.25
An	43.83	6.68	51.49	34.04	Al ^{VI}	0.26	0.21	0.25	0.26
Ab	55.33	92.91	47.19	64.69	Ti	0.21	0.18	0.2	0.21
Or	0.84	0.41	1.33	1.27	Fe ³⁺	0.49	0.51	0.49	0.46
					Fe ²⁺	1.7	1.71	1.97	1.93
					Mn	0.04	0.04	0.06	0.05
					Mg	2.52	2.69	2.32	2.32
					Ca	1.72	1.67	1.72	1.73
					Na	0.41	0.37	0.36	0.4
					K	0.16	0.12	0.15	0.18
					阳离子总量	15.51	15.49	15.51	15.54

从稀土元素配分型式分析(图8b),所有样品也显示出一致的曲线型式,轻稀土富集,重稀土亏损,弱的负Eu异常($\delta\text{Eu}=0.79\sim1.02$)。 $\Sigma\text{REE}=68.01\times10^{-6}\sim151.18\times10^{-6}$,稀土总量较低,变化范围窄。 $(\text{La/Yb})_{\text{N}}=8.17\sim16.66$,轻、重稀土分馏中等一强。 $(\text{Gd/Yb})_{\text{N}}=1.33\sim1.88$,重稀土分馏很弱,平坦的重稀土特征与典型的岛弧岩浆岩特征不同。

5 讨 论

5.1 花岗岩成因类型及源区特征

花岗闪长岩暗色矿物为角闪石及黑云母,富含闪长质包体,富钠(Na₂O在3.45%~4.96%),高钠钾比值(Na₂O/K₂O在1.33~2.52),P₂O₅与SiO₂较好的负相关性(图略),CIPW标准矿物计算中C分子<1,显示出I型花岗岩的特点(Chappell, 1974, 1999)。在岩石成因划分图解(Na₂O+K₂O)/CaO-(Zr+Nb+Ce+Y)(图9a)中,样品落在S/I造山花岗岩的范围

内,所以,查干乃呼都格花岗闪长岩具有I型花岗岩的特点。

从锆石Hf同位素分析,28个锆石点均具有负的 $\varepsilon_{\text{Hf}}(t)$ 值(-6.3~-2.0),平均值为-4.7,显示了以古老地壳熔融为主的特点。从锆石Hf二阶模式年龄分析, $T_{\text{DM2}}(\text{Ma})$ 为1437~1704 Ma(平均值为1606 Ma),显示了该岩石源区从亏损地幔中分离的时代为古一中元古代, $\varepsilon_{\text{Hf}}(t)-t$ 图解显示 $\varepsilon_{\text{Hf}}(t)$ 投点落在1.56 Ga(二阶模式年龄均值)演化线之上(图9c),反映了幔源岩浆或年轻地壳组分的参与;野外露头上闪长质包体与花岗闪长岩之间明显的化学混合,反映了壳幔混合作用;岩石中暗色矿物角闪石投点位于壳幔源范围之内(谢应雯和张玉泉,1990)(图9b),即源区可能有幔源岩浆参与。

因此,狼山地区查干乃呼都格早二叠世花岗闪长岩的成因类型为I型花岗岩,岩石主要来源于古一中元古代的古老地壳,源区明显受到幔源岩浆参与。

5.2 构造背景

对于狼山地区早二叠世的构造背景,学者们存在不同的认识。Wang et al.(2015, 2016)认为狼山地区早二叠世处于后碰撞的构造背景;刘烨(2012)对东升庙地区的花岗岩的研究表明,狼山地区早二叠世处于俯冲消减的构造背景。

本文研究的花岗闪长岩微量元素蛛网图显示富集大离子亲石元素K/Pb,不同程度的亏损高场强元素Nb/Ta/P/Ti的特点,稀土元素配分型式为轻稀土富集,重稀土亏损,弱的负Eu异常,反映了与岩浆弧相似的地球化学特征(Wilson, 1989),岩浆源区以古老地壳为主、幔源岩浆参与的特点可能反映了俯冲过程中地壳的加厚(Zhang et al., 2007)。所以,该岩浆岩的形成与俯冲作用有关。最近一些学者对狼山地区晚石炭世—早二叠世的岩体进行了岩石学及年代学研究,刘烨(2012)测得东升庙地区乌勒扎尔英云闪长岩的锆石²⁰⁶Pb/²³⁸U加权平均年龄为(304.0±3.4)Ma;皮桥辉等(2010)测得获各琦闪长岩的锆石²⁰⁶Pb/²³⁸U加权平均年龄为(273.9±1.2)Ma;Wang et al.(2015)测得沙尔楚鲁花岗闪长岩及狼山口的辉长闪长岩的锆石²⁰⁶Pb/²³⁸U加权平均年龄分别为(273.2±1.6)Ma和(272.6±2.3)Ma;项目组测得哈日陶勒盖石英闪长岩的(275.3±1.0)Ma,阿伦珠斯朗闪长岩的锆石²⁰⁶Pb/²³⁸U加权平均年龄(272.0±

表2 早二叠世花岗闪长岩主量元素(%)、微量元素和稀土元素(10^{-6})数据Table 2 Whole-rock major elements (%) and trace elements (10^{-6}) data of Early Permian granodiorite

样品号	5012-1	-P12-49-1	-P12-53-1	-P12-55-1	5101-1	-P12-43-1	-P12-43-2	-P12-43-3	-P12-45-1
SiO ₂	66.31	66.77	67.8	69.57	66.4	66.73	69.16	68.91	66.8
TiO ₂	0.41	0.42	0.36	0.34	0.45	0.37	0.31	0.37	0.42
Al ₂ O ₃	16.17	15.97	15.85	14.86	15.2	14.9	14.24	14.79	15.56
Fe ₂ O ₃	0.87	0.99	0.07	0.68	1.02	3.29	2.21	2.6	3.49
FeO	3.32	3.07	3.54	2.82	3.24	0.67	1.08	1.08	0.78
MnO	0.11	0.081	0.078	0.035	0.086	0.057	0.069	0.05	0.08
MgO	1.5	1.39	1.14	0.37	1.74	1.3	1.36	1.27	1.36
CaO	3.66	3.52	3.22	3.41	1.99	2.05	1.44	1.58	2.91
Na ₂ O	3.45	3.7	3.66	3.67	4.02	3.92	4.96	4.07	3.62
K ₂ O	2.6	2.23	2.51	2.71	2.8	2.49	1.97	2.75	2.36
P ₂ O ₅	0.12	0.1	0.091	0.083	0.11	0.096	0.079	0.091	0.11
烧失量	1.11	1.41	1.39	1.14	2.38	4.06	3	2.31	2.44
H ₂ O ⁺	0.85	1.63	1.33	0.71	1.27	1.86	2.21	1.74	1.79
CO ₂	0.24	0.62	0.59	1.1	0.98	18.42	7.63	5.41	4.84
总和	99.63	99.65	99.71	99.69	99.44	99.93	99.88	99.87	99.93
FeOT	4.10	3.96	3.60	3.43	4.16	3.63	3.07	3.42	3.92
Fe ₂ O ₃ T	4.56	4.40	4.00	3.81	4.62	4.03	3.41	3.80	4.36
Cs	1.82	1.44	1.51	1.39	2.1	3.04	2.49	1.85	2.38
Rb	96.3	76.9	75.4	89	108	58	85.6	52.3	97.8
Sr	454	416	419	388	425	312	335	431	420
Ba	555	805	555	965	2420	980	988	1140	1250
Ga	17	17.9	17.6	16.7	16.5	16	16.2	12.6	16
Nb	8.17	9.82	9.38	8.36	9	7.65	8.87	7.03	9.17
Ta	0.69	0.76	0.6	0.57	0.7	0.45	0.53	0.43	0.76
Zr	149	177	165	157	180	174	176	153	185
Hf	4	5.32	4.81	4.69	5.49	5.02	5.06	4.39	5.34
Th	10.2	10.1	7.83	8.98	9.18	7.48	8.42	5.21	9.54
V	64.1	46	46.1	39.6	50.2	33.7	37.6	31.8	30.7
Cr	9.5	6.24	5.57	5.26	7.32	4.83	9.98	4.45	6.68
Co	8.35	6.85	6.75	5.87	7.58	6.69	5.76	4.94	4.92
Ni	3.86	2.57	2.33	1.98	2.24	2.26	2.52	2.74	2.63
Li	25.9	21	20.8	21.2	21.4	12.7	25.4	17.6	21.9
Sc	11.1	9.87	9.16	7.9	12.4	10.4	9.16	7.21	9.44
U	0.85	1.05	0.94	0.86	1.98	1.29	1.07	1.21	2.04
Pb	14.2	15.3	14.2	14.2	14.4	13.7	12.9	9.59	10.9
Zn	48.5	57.3	56.6	54.3	55.3	67.8	73.5	46.2	46.4
Cu	5.92	4.92	3.80	7.88	6.23	3.64	4.81	6.27	3.80
La	20	29.1	27.1	27.6	23	31.5	30.2	13.5	27.4
Ce	37.1	56.7	46.5	47.6	43	54.3	51	23.2	47.2
Pr	4.37	6.24	5.66	5.56	5.39	6.15	5.92	2.91	5.43
Nd	15.8	22	20.6	19.7	20	21.8	20.6	10.8	18.8
Sm	3.03	4.12	3.75	3.54	3.76	3.82	3.5	2.06	3.21
Eu	0.83	0.98	0.94	0.99	1.18	1.1	0.89	0.64	0.92
Gd	2.76	3.53	3.31	3.11	3.32	3.39	2.95	1.84	2.71
Tb	0.43	0.64	0.59	0.52	0.57	0.55	0.47	0.31	0.45
Dy	2.43	3.55	3.18	2.95	3.14	2.88	2.45	1.64	2.44
Ho	0.5	0.71	0.63	0.56	0.62	0.56	0.48	0.33	0.48
Er	1.51	2.13	1.9	1.7	1.89	1.71	1.31	0.96	1.47
Tm	0.23	0.34	0.29	0.25	0.3	0.26	0.2	0.15	0.24
Yb	1.64	2.2	1.85	1.63	2.02	1.78	1.3	0.98	1.57
Lu	0.26	0.34	0.3	0.26	0.32	0.27	0.21	0.16	0.26
Y	14.8	18.6	16.5	15	16.2	14.6	11.6	8.53	12.2
Σ总量	105.69	151.18	133.10	130.97	124.71	144.67	133.08	68.01	124.78
LREE	81.13	119.14	104.55	104.99	96.33	118.67	112.11	53.11	102.96
HREE	24.56	32.04	28.55	25.98	28.38	26.00	20.97	14.90	21.82
LREE/HREE	3.30	3.72	3.66	4.04	3.39	4.56	5.35	3.56	4.72

表3 早二叠世花岗闪长岩锆石U-Pb定年数据

Table 3 Zircon LA-ICP-MS U-Pb data of Early Permian granodiorite

样品号	同位素比值						表面年龄/Ma					
	Pb	U	$^{232}\text{Th}/^{238}\text{U}$	1σ	$^{206}\text{Pb}/^{238}\text{U}$	1σ	$^{207}\text{Pb}/^{235}\text{U}$	1σ	$^{206}\text{Pb}/^{238}\text{U}$	1σ	$^{207}\text{Pb}/^{235}\text{U}$	1σ
TW5012-1												
1	18	355	0.54	0.0020	0.0470	0.0002	0.3440	0.0106	296	2	300	9
2	20	390	0.61	0.0004	0.0475	0.0003	0.3425	0.0046	299	2	299	4
3	10	199	0.55	0.0014	0.0475	0.0003	0.3463	0.0060	299	2	302	5
4	11	226	0.52	0.0059	0.0476	0.0003	0.3462	0.0060	300	2	302	5
5	13	259	0.54	0.0011	0.0474	0.0003	0.3413	0.0122	299	2	298	11
6	20	387	0.65	0.0014	0.0478	0.0003	0.3480	0.0034	301	2	303	3
7	18	356	0.54	0.0033	0.0477	0.0003	0.3447	0.0040	300	2	301	3
8	24	456	0.75	0.0024	0.0475	0.0003	0.3490	0.0033	299	2	304	3
9	12	237	0.59	0.0013	0.0476	0.0003	0.3481	0.0053	300	2	303	5
10	9	186	0.55	0.0026	0.0479	0.0003	0.3475	0.0072	301	2	303	6
11	11	219	0.61	0.0017	0.0474	0.0003	0.3425	0.0063	299	2	299	5
12	10	214	0.64	0.0010	0.0470	0.0003	0.3390	0.0120	296	2	296	11
13	11	218	0.55	0.0005	0.0473	0.0003	0.3448	0.0075	298	2	301	7
14	11	212	0.74	0.0017	0.0472	0.0003	0.3456	0.0054	297	2	301	5
15	7	138	0.54	0.0029	0.0474	0.0003	0.3461	0.0134	299	2	302	12
16	14	289	0.60	0.0023	0.0475	0.0003	0.3444	0.0047	299	2	300	4
17	7	153	0.49	0.0003	0.0476	0.0003	0.3406	0.0068	300	2	298	6
18	15	300	0.60	0.0043	0.0477	0.0003	0.3445	0.0039	300	2	301	3
19	11	236	0.46	0.0003	0.0475	0.0003	0.3489	0.0058	299	2	304	5
20	14	277	0.53	0.0037	0.0474	0.0003	0.3425	0.0064	299	2	299	6
21	12	240	0.43	0.0028	0.0477	0.0003	0.3427	0.0050	300	2	299	4
22	24	473	0.43	0.0016	0.0475	0.0003	0.3438	0.0037	299	2	300	3
23	11	220	0.44	0.0009	0.0477	0.0003	0.3461	0.0071	300	2	302	6
24	14	282	0.41	0.0008	0.0480	0.0003	0.3457	0.0056	302	2	301	5
TW5101-1												
1	18	373	0.53	0.0009	0.0466	0.0005	0.3342	0.0056	294	3	293	5
2	25	485	0.57	0.0009	0.0460	0.0005	0.5620	0.0139	290	3	453	11
3	21	453	0.52	0.0039	0.0460	0.0005	0.3293	0.0053	290	3	289	5
4	21	449	0.54	0.0005	0.0462	0.0005	0.3359	0.0064	291	3	294	6
5	22	473	0.74	0.0008	0.0451	0.0004	0.3258	0.0061	285	3	286	5
6	19	405	0.61	0.0074	0.0467	0.0005	0.3409	0.0058	294	3	298	5
7	21	422	0.66	0.0008	0.0470	0.0005	0.3443	0.0055	296	3	300	5
8	26	542	0.58	0.0018	0.0464	0.0005	0.3403	0.0051	292	3	297	4
9	23	485	0.56	0.0011	0.0462	0.0005	0.3322	0.0052	291	3	291	5
10	22	476	0.49	0.0029	0.0454	0.0005	0.3261	0.0052	286	3	287	5
11	24	498	0.55	0.0015	0.0476	0.0005	0.3478	0.0057	300	3	303	5
12	19	399	0.57	0.0007	0.0472	0.0005	0.3455	0.0059	297	3	301	5
13	24	503	0.60	0.0022	0.0465	0.0005	0.3325	0.0052	293	3	291	5
14	21	462	0.54	0.0014	0.0464	0.0005	0.3377	0.0056	292	3	295	5
15	32	682	0.57	0.0008	0.0466	0.0005	0.3428	0.0054	293	3	299	5
16	24	466	0.54	0.0017	0.0510	0.0006	0.4040	0.0075	320	4	345	6
17	27	556	0.58	0.0015	0.0479	0.0005	0.3353	0.0053	301	3	294	5
18	18	387	0.50	0.0004	0.0474	0.0005	0.3417	0.0056	299	3	298	5
19	29	610	0.61	0.0016	0.0460	0.0005	0.3554	0.0053	290	3	309	5
20	26	551	0.69	0.0102	0.0458	0.0005	0.3356	0.0051	288	3	294	4
21	28	606	0.58	0.0035	0.0453	0.0005	0.3261	0.0049	286	3	287	4
22	19	401	0.50	0.0005	0.0470	0.0005	0.3415	0.0054	296	3	298	5
23	25	511	0.55	0.0008	0.0478	0.0005	0.3412	0.0056	301	3	298	5
24	28	564	0.61	0.0018	0.0472	0.0005	0.3470	0.0051	297	3	302	4

表4 早二叠世花岗闪长岩锆石Hf同位素数据

Table 4 Zircon Hf isotopic composition of Early Permian U-Pb data of granodiorite

样品	年龄 /Ma	$^{176}\text{Yb}/^{177}\text{Hf}$ (corr)	$^{176}\text{Lu}/^{177}\text{Hf}$ (corr)	$^{176}\text{Hf}/^{177}\text{Hf}$ (corr)	2σ	$\varepsilon_{\text{Hf}}(0)$	$\varepsilon_{\text{Hf}}(t)$	2s	T_{DMI}/Ma	2s	$f_{\text{Lu/Hf}}$	T_{DM2}/Ma
TW5012-1.1	299	0.0468	0.0012	0.282460	0.000018	-11.0	-4.7	0.6	1128	51	-0.96	1610
TW5012-1.2	299	0.0528	0.0013	0.282472	0.000022	-10.6	-4.3	0.8	1112	61	-0.96	1584
TW5012-1.3	299	0.0242	0.0006	0.282436	0.000020	-11.9	-5.4	0.7	1143	55	-0.98	1656
TW5012-1.4	299	0.0233	0.0006	0.282472	0.000020	-10.6	-4.2	0.7	1094	55	-0.98	1576
TW5012-1.5	299	0.0361	0.0010	0.282420	0.000016	-12.5	-6.1	0.6	1176	45	-0.97	1696
TW5012-1.6	299	0.0355	0.0010	0.282439	0.000018	-11.8	-5.4	0.6	1150	51	-0.97	1654
TW5012-1.7	299	0.0245	0.0007	0.282455	0.000018	-11.2	-4.8	0.6	1119	50	-0.98	1614
TW5012-1.8	299	0.0303	0.0009	0.282496	0.000017	-9.8	-3.4	0.6	1068	48	-0.97	1526
TW5012-1.9	299	0.0401	0.0012	0.282496	0.000020	-9.7	-3.4	0.7	1074	55	-0.97	1527
TW5012-1.10	299	0.0300	0.0009	0.282440	0.000018	-11.7	-5.3	0.6	1146	50	-0.97	1650
TW5012-1.11	299	0.0276	0.0009	0.282436	0.000019	-11.9	-5.5	0.7	1150	53	-0.97	1659
TW5012-1.12	299	0.0325	0.0010	0.282474	0.000023	-10.5	-4.2	0.8	1101	64	-0.97	1576
TW5012-1.13	299	0.0243	0.0008	0.282439	0.000015	-11.8	-5.4	0.5	1144	43	-0.98	1651
TW5012-1.14	299	0.0353	0.0010	0.282480	0.000016	-10.3	-4.0	0.6	1092	45	-0.97	1562
TW5012-1.15	299	0.0213	0.0006	0.282470	0.000019	-10.7	-4.2	0.7	1094	54	-0.98	1579
Tw5101-1.1	293	0.0298	0.0010	0.282418	0.000018	-12.5	-6.3	0.6	1181	51	-0.97	1704
Tw5101-1.2	293	0.0311	0.0009	0.282453	0.000018	-11.3	-5.0	0.6	1128	50	-0.97	1625
Tw5101-1.3	293	0.0197	0.0006	0.282438	0.000016	-11.8	-5.5	0.6	1141	44	-0.98	1655
Tw5101-1.4	293	0.0262	0.0008	0.282503	0.000016	-9.5	-3.2	0.6	1055	44	-0.97	1512
Tw5101-1.5	293	0.0339	0.0011	0.282461	0.000016	-11.0	-4.8	0.6	1122	45	-0.97	1609
Tw5101-1.6	293	0.0348	0.0012	0.282460	0.000018	-11.0	-4.8	0.6	1127	51	-0.96	1613
Tw5101-1.7	293	0.0381	0.0012	0.282469	0.000018	-10.7	-4.5	0.6	1114	50	-0.96	1593
Tw5101-1.8	293	0.0359	0.0011	0.282452	0.000017	-11.3	-5.1	0.6	1136	48	-0.97	1629
Tw5101-1.9	293	0.0452	0.0014	0.282426	0.000017	-12.2	-6.1	0.6	1180	47	-0.96	1690
Tw5101-1.10	293	0.0404	0.0012	0.282432	0.000016	-12.0	-5.8	0.6	1167	47	-0.96	1675
Tw5101-1.11	293	0.0235	0.0008	0.282464	0.000015	-10.9	-4.6	0.5	1109	42	-0.98	1599
Tw5101-1.12	293	0.0387	0.0012	0.282505	0.000020	-9.4	-3.2	0.7	1063	55	-0.96	1512
Tw5101-1.13	293	0.0419	0.0013	0.282539	0.000020	-8.2	-2.0	0.7	1017	57	-0.96	1437

2.0 Ma)^①。由此可见,狼山地区晚石炭世—早二叠世侵入岩岩石组合为闪长岩+石英闪长岩+花岗闪长岩(英云闪长岩),与陆缘弧的岩石组合一致。

有意义的是,测区发育的早—中二叠世大石寨组底部的玄武安山岩锆石 $^{206}\text{Pb}/^{238}\text{U}$ 加权平均年龄为(285.0 ± 2.3) Ma^①,顶部的英安岩锆石 $^{206}\text{Pb}/^{238}\text{U}$ 加权平均年龄为(270.0 ± 1.0) Ma^①,火山岩组合为玄武岩+玄武安山岩+安山岩+英安岩^①,与测区同时代的侵入岩相对应。因此,早二叠世测区处于大陆边缘弧的构造背景。

近年来的研究表明,狼山地区存在早古生代弧岩浆岩,测得早志留世片麻状石英闪长岩的锆石年龄为(443.9 ± 2.4) Ma~(440 ± 1) Ma(Wang et al., 2015;

滕学建等,2019),那么,晚石炭世—早二叠世发育的陆缘弧岩浆岩是否为持续俯冲作用的产物?答案是否定的。首先,早志留世岩浆岩发育典型的片麻状构造,而晚石炭世—早二叠世岩浆岩为块状构造;其次,早志留世岩浆岩仅发育在古元古代宝音图岩群中,而晚石炭—早二叠世则在古元古代宝音图岩群及中元古代渣尔泰山群中广泛发育,反映了两者并非同一构造背景下的产物。由此可见,早古生代晚期狼山地区可能经历了弧陆拼贴或增生作用,这一认识得到了 Wang et al.(2015)的支持,即狼山地区善岱庙地区二云母二长花岗岩的锆石年龄为(418.0 ± 2.3) Ma(图2),反映了同造山拼贴作用的构造背景。

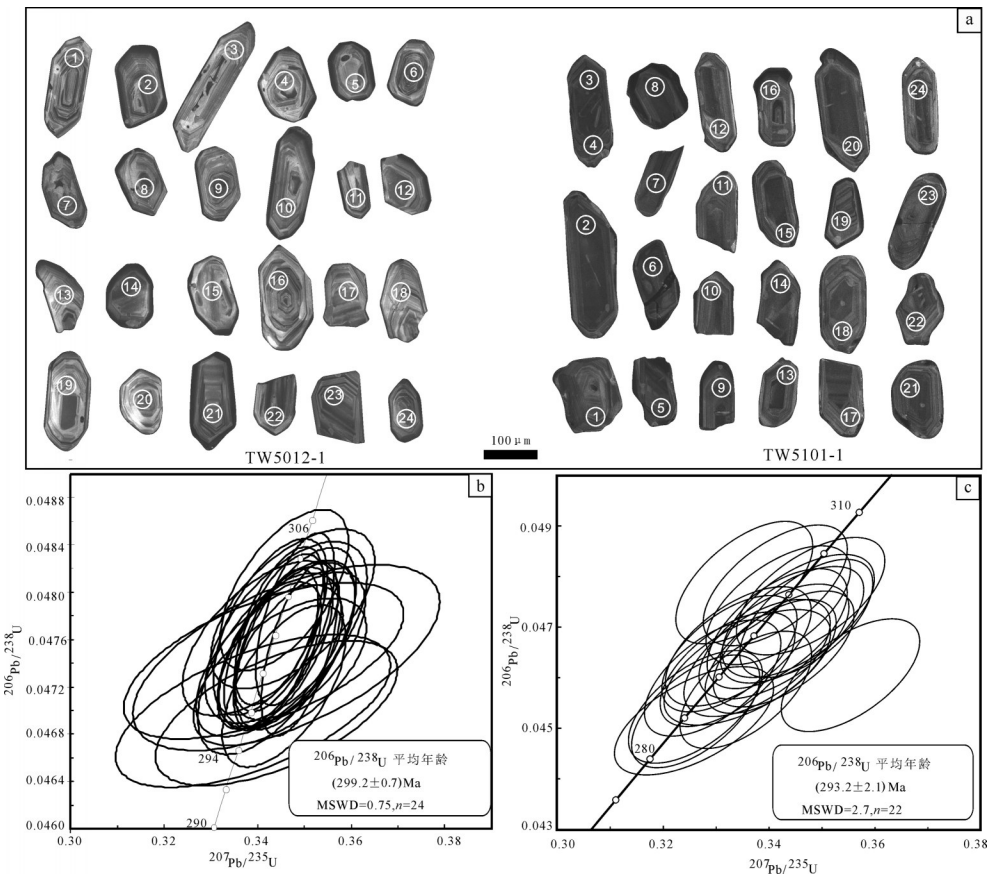


图6 花岗闪长岩的锆石CL图像(a)和锆石U-Pb年龄谐和图(b、c)
Fig.6 CL images of zircons(a), $^{206}\text{Pb}/^{238}\text{U}$ average age and concordia plots of zircons from granodiorite (b, c)

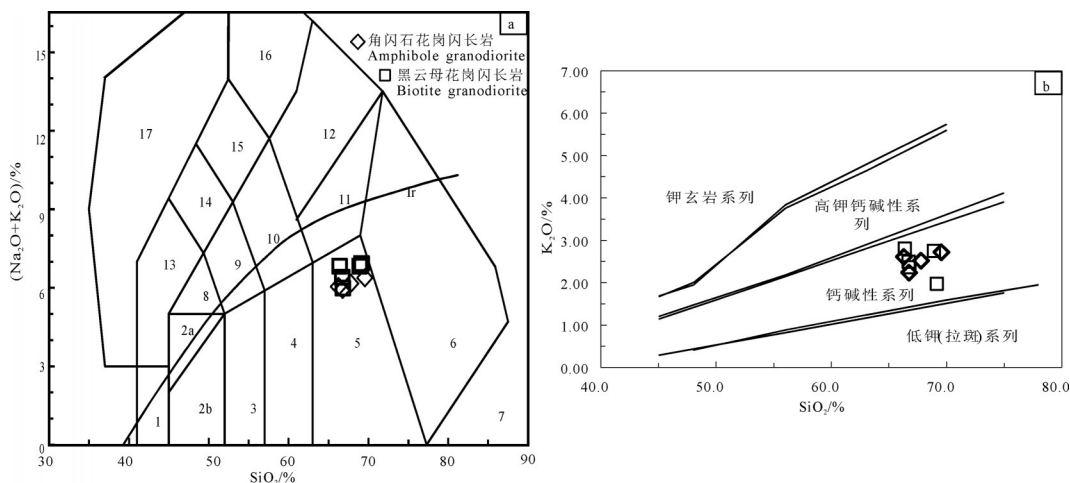


图7早二叠世花岗闪长岩主量元素分类图
侵入岩的TAS图解(a)(据Middlemost, 1994);AFM图解(b)(据Kuno, 1968)
1—橄榄辉长岩; 2a—碱性辉长岩; 2b—亚碱性辉长岩; 3—辉长闪长岩; 4—闪长岩; 5—花岗闪长岩; 6—花岗岩; 7—硅英岩; 8—二长辉长岩; 9—二长闪长岩; 10—二长岩; 11—石英二长岩; 12—正长岩; 13—副长石辉长岩; 14—副长石二长闪长岩; 15—副长石二长正长岩; 16—副长正长岩; 17—副长深成岩

Fig. 7 Classification diagrams of major elements TAS diagram of intrusive rock (a) (after Middlemost, 1994); AFM diagram (b) (after Kuno, 1968)
1—Olivine gabbro; 2a—Alkaline gabbro; 2b—Subalkaline gabbro; 3—Gabbro; 4—Diorite; 5—Granodiorite; 6—Granite; 7—Silcrite; 8—Monzonite gabbro; 9—Monzonite diorite; 10—Monzonite; 11—Quartz monzonite; 12—Syenite; 13—Feldspathoid gabbro; 14—Feldspathoid monzonite diorite; 15—Feldspathoid monzonite syenite; 16—Feldspathoid syenite; 17—Feldspathoid pluton

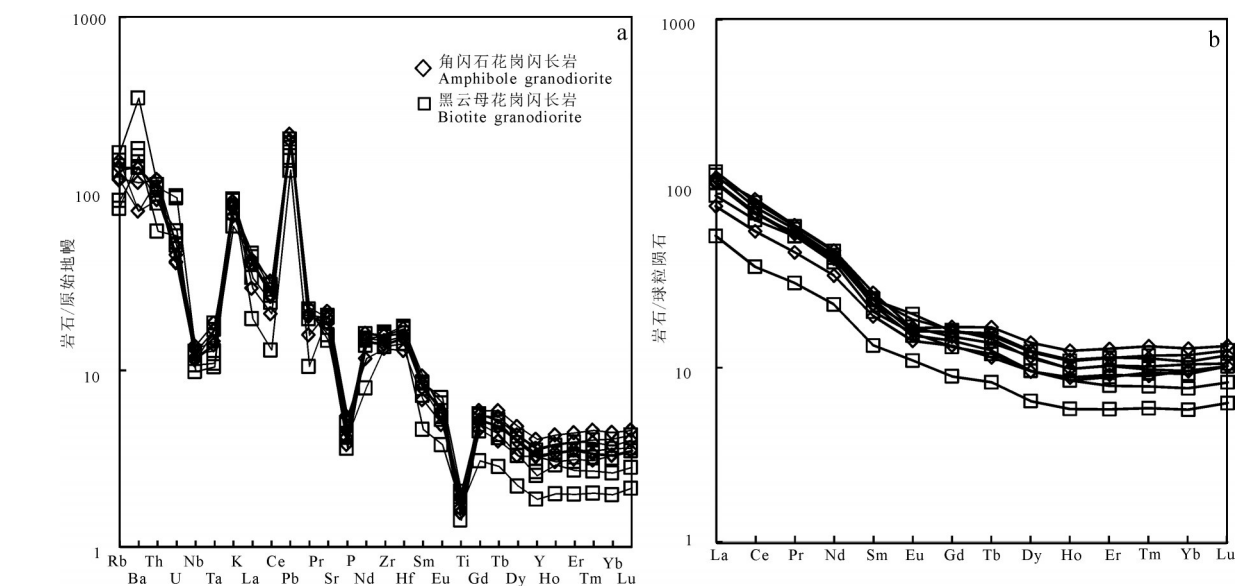


图8早二叠世花岗闪长岩微量元素蛛网图(a)及稀土元素配分曲线(b)(据Sun and McDonough, 1989)
原始地幔及球粒陨石标准化值据Sun and McDonough(1989)

Fig. 8 Primitive mantle-normalized trace element spidergrams(a) and chondrite-normalized REE patterns (b)
Standardized values of primitive mantle and chondrite after Sun and McDonough (1989)

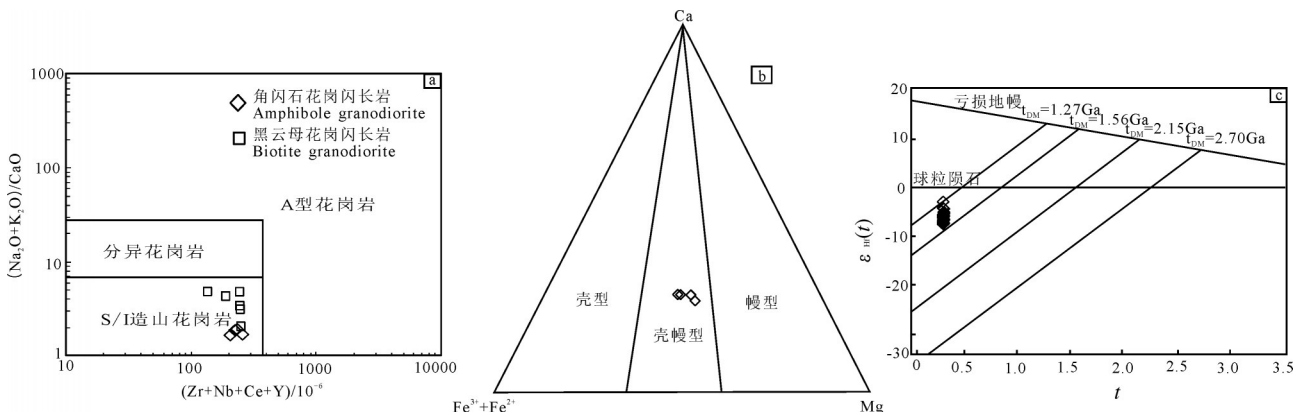


图9 花岗闪长岩成因判别图解
a—(Na₂O+K₂O)/CaO—(Zr+Nb+Ce+Y)图解(据Whalen et al., 1987); b—角闪石成因图解(据谢应雯和张玉泉, 1990); c— $t-\varepsilon_{\text{Mg}}(t)$ 演化图
(据Yang et al., 2006)

Fig. 9 Genetic discrimination diagrams for granodiorites

a—(Na₂O+K₂O)/CaO—(Zr+Nb+Ce+Y) diagram (after Whalen et al., 1987); b—Genetic diagram of amphiboles
(after Xie Yinewen and Zhang Yuquan, 1990); c— $t-\varepsilon_{\text{Mg}}(t)$ diagram (after Yang et al., 2006)

可对比的是,在华北地块北缘中东部,也陆续报道了晚石炭世—早二叠世侵入岩。Zhang et al. (2007, 2009a, 2009b)指出,华北地块北缘晚石炭世—早二叠世侵入岩与俯冲作用有关;张维等(2012)、吴飞等(2014)对固阳地区早二叠世的侵入岩进行了研究,岩石组合主要为闪长岩、石英闪长岩、花岗

闪长岩,认为其形成于大陆边缘弧环境。因此,狼山地区与华北地块北缘中东部晚石炭世—早二叠世的侵入岩岩石组合一致,均具有陆缘弧的岩石组合特征,可能反映了相同的构造背景。

综上所述,狼山地区早二叠世处于陆缘弧的构造背景,华北地块北缘早二叠世存在广泛的俯冲作用。

6 结 论

(1) 狼山地区早二叠世花岗闪长岩的锆石 $^{206}\text{Pb}/^{238}\text{U}$ 加权平均年龄(299 ± 1)~(293 ± 2) Ma, 岩石暗色矿物为角闪石及黑云母, 富含闪长质包体, 富钠(Na_2O 在3.45%~4.96%), 高钠钾比值($\text{Na}_2\text{O}/\text{K}_2\text{O}$ 在1.33~2.52), 成因类型为I型花岗岩, Hf同位素及微量元素特征表明岩石主要为古一中元古代陆壳熔融, 源区明显受到幔源岩浆参与。

(2) 狼山地区早二叠世处于陆缘弧的构造背景, 其侵入岩岩石组合及反映的构造背景与华北地块北缘中东部可以对比。

致谢:本文在写作过程中得到了赵风清研究员、辛后田教授级高级工程师的建议,在此表示衷心的感谢!

注释

①天津地质调查中心. 2016. 区域地质矿产调查报告(查干呼舒庙等六幅)[R].

References

- Allen M B, Windley B F, Zhang C. 1993. Palaeozoic collisional tectonics and magmatism of the Chinese Tien Shan, Central Asia[J]. *Tectonophysics*, 220(1/4): 89–115.
- Allen M B, Engor A M C, Natalin B A. 1995. Junggar, Turfan and Alakol basins as Late Permian to Early Triassic extensional structures in a sinistral shear zone in the Altai orogenic collage. Central Asia[J]. *Journal of the Geological Society (London)*, 152 (2): 32–338.
- Chappell B W, White A J R. 1974. Two contrasting granite types [J]. *Pacific Geology*, 8:173–174.
- Chappell B W. 1999. Aluminium saturation in I- and S-type granites and the characterization of fractionated haplogranites [J]. *Lithos*, 46:535–551.
- Coleman R G. 1989. Continental growth of Northwest China [J]. *Tectonics*, 8(3): 621–635.
- Dong Hongkai, Meng Qingtao, Liu Guang, Duan Xianle, Ti Zhenhai, Zhu Wei, Xue Pengyuan, Cheng Haifeng, Ji Tianyi. 2018. Geochemical characteristics of Early Silurian granite from Biaoshan area in Beishan, Inner Mongolia and their tectonic implications[J]. *Northwestern Geology*, 51(1):159–174(in Chinese with English abstract).
- Feng Lixia, Zhang Zhicheng, Han Baofu, Ren Rong, Li Jianfeng, Su Li. 2013. LA-ICP-MS zircon U-Pb ages of granitoids in Darhan Mumigangan Joint Banner, Inner Mongolia, and their geological significance[J]. *Geol. Bull. China*, 32:1737–1748 (in Chinese with English abstract).
- English abstract).
- Gao J, Li M S, Xiao X C, Tang Y Q and He G Q. 1998. Paleozoic tectonic evolution of the Tianshan orogen, northwestern China[J]. *Tectonophysics*, 287(1/4): 213–231.
- Griffin W L, Pearson N J, Belousova E, Jackson S E, Van Achterbergh E, O'Reilly S Y, Shee S R. 2000. The Hf isotope composition of cratonic mantle: LAM-MC-ICPMS analysis of zircon megacrysts in kimberlites [J]. *Geochimica et Cosmochimica Acta*, 64(1): 133–147.
- Guo Xiyun, Sun Huashan, Dong Beiguan, Ren Jianxun, Xu Ruiying, Gao Bo. 2019. Dating and genesis of Early Permian granitoids in the north of Xilinhhot, Inner Mongolia[J]. *Geology in China*, 46(6): 1396–1409(in Chinese with English abstract).
- Han B F, He G Q, Wang X C, Guo Z J. 2011. Late Carboniferous collision between the Tarim and Kazakhstan-Yili terranes in the western segment of the South Tian Shan Orogen, Central Asia, and implications for the Northern Xinjiang, western China[J]. *Earth-Sci. Rev.*, 109: 74–93.
- Jahn B M, Griffin W L, Windley B F. 2000. Continental growth in the Phanerozoic: Evidence from Central Asia [J]. *Tectonophysics*, 328 (1):vii–x.
- Kuno H. 1968. Differentiation of basaltic magmas[C]//Hess H H & Poldervaart, A(eds.). Basalts: The Poldervaart treatise on rocks of basaltic composition, v. 2. Interscience, New York, p. 623–688.
- Liu M, Zhang D, Xiong G Q, Zhao H T, Di Y J, Wang Z, Zhou Z G. 2016. Zircon U-Pb age Hf isotope and geochemistry of Carboniferous intrusions from the Langshan area, Inner Mongolia: Petrogenesis and tectonic implications [J]. *Journal of Asian Earth Sciences*, 120:139–158.
- Li Huaijun, Geng Jianzhen, Hao Shuan, Zhang Yongqing, Li Huiming. 2009. Study on the using LA-MC-ICPMS to date the U-Pb isotopic age of zircons[J]. *Bulletin of Mineralogy, Petrology and Geochemistry*, 28 (Supp.) :77 (in Chinese)
- Liu Ye. 2012. Geochemical and Chronological Characteristics of the Granitic Gneisses and Intrusive Rocks from Dongshengmiaozhuang Region, Inner Mongolia and Their Tectonic Implications[D]. Lanzhou: Lanzhou University (in Chinese with English abstract).
- Liu Y S, Gao S, Hu Z C. 2010. Continental and oceanic crust recycling-induced melt-peridotite interactions in the Trans-North of mantle xenoliths[J]. *Journal of Petrology*, 51:537–571.
- Ludwig K R. 2003. Users manual for Isoplot 3.0: A Geochronological Toolkit for Microsoft Excel[M]. Berkeley: Berkeley Geochronology Center, California:1–39.
- LÜ Daxin, LÜ Hongjie. 2018. Zircon U-Pb age of monzonite granite from Abag Banner in Inner Mongolia and its tectonic significance[J]. *Northwestern Geology*, 51(2):37–45 (in Chinese with English abstract).
- Middlemost E A K. 1994. Naming materials in the magma/igneous rock system[J]. *Earth-Science Reviews*, 37(3/4):215–224.

- Peng R M, Zhai Y S, Li C S, Ripley E M. 2013. The Erbutu Ni–Cu deposit in the Central Asian Orogenic Belt: A Permian magmatic sulfide deposit related to Boninitic magmatism in an arc setting [J]. *Econ. Geol.*, 108:1879–1888.
- Pi Qiaohui, Liu Changzheng, Chen Yuelong, Li Yongquan, Li Dapeng. 2010. Formation epoch and genesis of intrusive rocks in Huogeqi orrefield of Inner Mongolia and their relationship with copper mineralization [J]. *Mineral Deposits*, 29(3):437–451 (in Chinese with English abstract).
- Sengor A M C, Natalin B A, Burtman V S. 1993. Evolution of the Altaiid tectonic collage and Palaeozoic crustal growth in the Eurasia[J]. *Nature*, 364: 299–304.
- Sun S S, McDonough W F. 1989. Chemical and isotopic systematics of oceanic basalts: Implications for mantle composition and processes[C]//Saunders A D, Norry M J (eds.). *Magmatism in the Ocean Basins*. Geological Society, London, Special Publications, 42 (1): 313–345.
- Teng Xuejian, Tian Jian, Liu Yang, Zhang Yong, Teng Fei, Duan Xiaolong. 2019. Definition and geological significance of Early Silurian quartz diorite pluton in Langshan area, Inner Mongolia[J]. *Earth Science*, 44(4): 1236–1247 (in Chinese with English abstract).
- Wang Wenlong, Teng Xuejian, Liu Yang, Teng Fei, Guo Shuo, He Peng, Tian Jian, Duan Xiaolong. 2017. Zircon U–Pb chronology and geological characteristics of the Wuheertu granite mass in Langshan, Inner Mongolia[J]. *Journal of Geomechanics*, 23 (3): 382–396 (in Chinese with English abstract).
- Wang Z Z, Han B F, Feng L X, Liu B. 2015. Geochronology, geochemistry and origins of the Paleozoic–Triassic plutons in the Langshan area, western Inner Mongolia, China[J]. *Asian Earth Sci.*, 97:337–351
- Wang Z Z, Han B F, Feng L X, Liu B, Zheng B, Kong L J. 2016. Tectonic attribution of the Langshan area in western Inner Mongolia and implications for the Neorarchean–Paleoproterozoic evolution of the Western North China Craton: Evidence from LA–ICP–MS zircon U–Pb dating of the Langshan basement [J]. *Lithos*, 261: 278–295.
- Whalen J B, Currie K L, Chappell B W. 1987. A–type granites geochemical characteristics, discrimination and petrogenesis[J]. *Contribution to Mineralogy and Petrology*, 95: 407–419.
- Wilson M. 1989. Igneous Petrogenesis [M]. London: Unwin Hyman, 1–466.
- Windley B F, Allen M B, Zhang C, Zhao Z Y, Wang G R. 1990. Paleozoic accretion and Cenozoic reformation of the Chinese Tien Shan range, Central Asia [J]. *Geology*, 18(2): 128–131.
- Windley B F, Alexeiev D, Xiao W J, Kröner A, Badarch G. 2007. Tectonic models for accretion of the Central Asian Orogenic Belt [J]. *J. Geol. Soc., Lond.* 164: 31–47.
- Wu Fei, Zhang Shuanghong, Zhao Yue, Ye Hao. 2014. Emplacement depth and tectonic significance of Early Permian pluton in Inner Mongolia Guyang area, northern margin of North China block [J]. *Geology in China*, 41(3):824–837 (in Chinese with English abstract).
- Wu F Y, Yang Y H, Xie L W, Yang J H, Xu P. 2006. Hf isotopic compositions of the standard zircons and baddeleyites used in U–Pb geochronology [J]. *Chemical Geology*, 234(1/2): 105–126.
- Wu T R, He G Q, Zhang C. 1998. On Paleozoic tectonics in the Alxa region, Inner Mongolia, China [J]. *Acta Geol. Sin.*, 72: 256–263.
- Xiao W J, Windley B F, Badarch G, Sun S, Li J L, Qin K Z, Wang Z H. 2004. Palaeozoic accretionary and convergent tectonics of the southern Altaids: Implications for the growth of Central Asia [J]. *Journal of the Geological Society*, 161(3): 339–342.
- Xiao W J, Mao Q G, Windley B F, Han C M, Qu J F, Zhang J E, Ao S J, Guo Q Q, Cleven N R, Lin S F, Shan Y H, Li J L. 2010. Paleozoic multiple accretionary and collisional processes of the Beishan orogenic collage [J]. *Am. J. Sci.* 310: 1553–1594.
- Xie Jianqiang, Di Pengfei, Yang Jing, Chen Wanfeng, Wei Haifeng, Zhai Xinwei. 2018. LA–ICP–MS zircon U–Pb age, geochemistry and tectonic implications of metamorphic dacite from Huaniushan Group in Beishan area, Gansu, China[J]. *Northwestern Geology*, 51 (1):54–64(in Chinese with English abstract).
- Xie Yingwen, Zhang Yuquan. 1990. Peculiarities and genetic significance of hornblende from granite in the Hengduanshan region [J]. *Acta Mineralogica Sinica*, 10(1):36–45 (in Chinese with English abstract).
- Xu B, Charvet J, Chen Y, Zhao P, Shi G Z. 2013. Middle Paleozoic convergent orogenic belts in western Inner Mongolia (China): Framework, kinematics, geochronology and implications for tectonic evolution of the Central Asian Orogenic Belt[J]. *Gondwana Res.*, 23:1342–1364.
- Xu Z, Han B F, Ren R, Zhou Y Z, Zhang L, Chen J F, Su L, Li X H, Liu D Y. 2012. Ultramafic–mafic mélange, island arc and post-collisional intrusions in the Mayile Mountain, West Junggar, China: Implications for Paleozoic intraoceanic subduction–accretion process [J]. *Lithos*, 132–133: 141–161.
- Yang J H, Wu F Y, Shao J A, Wilde S A, Liu X M. 2006. Constrains on the timing of the Yanshan fold and thrust belt, North China[J]. *Earth Planet. Sci. Lett.*, 246: 336–352
- Zhang W, Jian P, Kröner A, Shi, Y R. 2013. Magmatic and metamorphic development of an early to mid- Paleozoic continental margin arc in the southernmost Central Asian Orogenic Belt, Inner Mongolia, China[J]. *Asian Earth Sci.*, 72:63–74.
- Zhang S H, Zhao Y, Song B, Yang Z Y, Hu J M, Wu H. 2007. Carboniferous granitic plutons from the northern margin of the North China block: Implications for a Late Paleozoic active continental margin[J]. *J. Geol. Soc. Lond.*, 164: 451–463.
- Zhang S H, Zhao Y, Song B, Hu J M, Liu S W, Yang H Y, Chen F K, Liu X M, Liu J. 2009. Contrasting Late Carboniferous and Late Permian–Middle Triassic intrusive suites from the northern margin of the North China craton: Geochronology, petrogenesis,

- and tectonic implications[J]. Geol. Soc. Am. Bull., 121:181–200.
- Zhang S H, Zhao Y, Kroner A, Liu X M, Xie L W, Chen F K. 2009b. Early Permian plutons from the northern North China Block: Constraints on continental arc evolution and convergent margin magmatism related to the Central Asian Orogenic Belt[J]. Int. J. Earth Sci., 98:1441–1467.
- Zhang Wei, Jian Ping. 2012. SHRIMP dating of the Permian Guyang diorite–granodiorite–tonalite suite in the northern margin of the North China Craton[J]. Geology in China, 39(6):1593–1603 (in Chinese with English abstract).
- Zhang X H, Gao Y L, Wang Z J, Liu H, Ma Y G. 2012. Carboniferous appinitic intrusions from the northern North China craton: geochemistry, petrogenesis and tectonic implications[J]. J. Geol. Soc., Lond., 169: 337–351.
- Zhao Chuang, Su Xuliang, Xue Bin, Cheng Dongjiang, Shi Xingjun, Song Taotao, Zhang Kuo. 2020. Zircon U–Pb dating and geochemical characteristics of granites in the area of Wula-Yingba, Kuchu, western Inner Mongolia[J]. Geology in China, <http://141.rm.cglhub.com/kcms/detail/11.1167..20200210.2231.004.html>.
- 李怀坤, 耿建珍, 郝爽, 张永清, 李惠民. 2009. 用激光烧灼多接收器等离子体质谱仪 (LA-MC-ICPMS) 测定锆石 U-Pb 同位素年龄的研究[J]. 矿物岩石地球化学通报, 28(增刊): 77.
- 刘烨. 2012. 内蒙古东升庙地区花岗片麻岩和侵入岩的地球化学、年代学特征及构造意义[D]. 兰州: 兰州大学.
- 皮桥辉, 刘长征, 陈岳龙, 李泳泉, 李大鹏. 2010. 内蒙古霍各乞海西期侵入岩形成时代、成因及其与铜矿体的关系[J]. 矿床地质, 29(3): 437–451.
- 滕学建, 田健, 刘洋, 张永, 滕飞, 段霄龙. 2019. 内蒙古狼山地区早志留世石英闪长岩体的厘定及其地质意义[J]. 地球科学, 44(4): 1236–1247.
- 王文龙, 滕学建, 刘洋, 滕飞, 郭硕, 何鹏, 田健, 段霄龙. 2019. 内蒙古狼山乌和尔图花岗岩体锆石 U-Pb 年代学及地球化学特征[J]. 地质力学学报, 23(3): 382–396.
- 吴飞, 张拴宏, 赵越, 叶浩. 2014. 华北地块北缘内蒙古固阳地区早二叠世岩体的侵位深度及其构造意义[J]. 中国地质, 41(3): 824–837.
- 谢应雯, 张玉泉. 1990. 横断山区花岗岩类中角闪石的标型特征及其成因意义[J]. 矿物学报, 10(1): 36–45.
- 张维, 简平. 2012. 华北北缘固阳二叠纪闪长岩–石英闪长岩–英云闪长岩套 SHRIMP 年代学[J]. 中国地质, 39(6): 1593–1603.
- 赵闯, 苏旭亮, 薛斌, 程东江, 史兴俊, 宋涛涛, 张阔. 2020. 内蒙古西部苦楚乌拉–英巴地区花岗岩锆石 U-Pb 定年及地球化学特征[J]. 中国地质, <http://141.rm.cglhub.com/kcms/detail/11.1167..20200210.2231.004.html>. (CNKI 网络首发)